



## SCENARIO SHAKEMAPS FOR USE IN EARTHQUAKE RISK STUDIES IN MONTREAL

### Hadi Ghofrani

Post-doctoral fellow, Western University, Canada  
*hghofra@uwo.ca*

### Gail M. Atkinson

Professor of Earth Sciences, Western University, Canada  
*gmatkinson@aol.com*

### Luc Chouinard

Professor of Civil Engineering, McGill University, Canada  
*luc.chouinard@mcgill.ca*

### Philippe Rosset

Associate researcher, McGill University, Canada  
*philippe.rosset@mail.mcgill.ca*

### Kristy F. Tiampo

Professor of Earth Sciences, Western University, Canada  
*ktiampo@uwo.ca*

**ABSTRACT:** Montreal ranks second after Vancouver among Canadian urban areas in terms of seismic risk. Variability in near surface geology plays an important role in earthquake ground shaking in the region. We constructed scenario shakemaps for Montreal using forecasts of most-likely earthquake locations, combined with recent ground motion modelling, validated with local recorded data and soil information specific to the region. We used microzonation information from Montreal to assess the expected site amplification effects. The target probability level for the scenarios is near the 2%/50 yr ground motions, as used for design of new structures in Montreal according to the National Building Code of Canada (NBCC 2010). Scenario shakemaps are generated to study the expected ground-shaking intensity distribution patterns for input to damage and risk studies. The impact of event location on expected ground motions and intensities was tested by considering the occurrence of a scenario (a given magnitude event) at various locations in the region. The results of this study may be used as input to seismic risk studies for Montreal.

### 1. Introduction

Shakemaps (Wald et al. 1999) are maps that show the spatial distribution of recorded and estimated peak ground motions and estimate the corresponding felt-intensity at locations throughout a region, for purposes of providing rapid public planning and emergency response information in the immediate aftermath of local and regional earthquakes. Shakemap uses ground motion prediction equations (GMPEs) to estimate ground motion at locations over a spatial grid, and combines these calculated motions with recordings to produce an interpreted map of the intensity of shaking. intensity of ground shaking. Macroseismic intensity can be determined by using empirical correlations between instrumental ground motion and felt intensity (e.g. Atkinson and Kaka 2007; Worden et al. 2012).

For planning purposes and risk studies, scenario shakemaps, which predict the expected ground shaking patterns for a specified earthquake magnitude and location, are very useful. Scenario shakemaps have applications in earthquake engineering, seismological research, emergency response planning, reliability analysis of utilities, public information, and education (Wald et al. 2007). While no scenario will prove accurate in every detail, scenario shakemaps are useful for providing a regional pattern of expected damage and to give a more complete understanding of earthquake hazards; this is a first step toward developing earthquake response plans.

The purpose of this study is to construct scenario shakemaps for Montreal using forecasts of most-likely earthquake locations, combined with ground motion models validated with local recorded data and soil information specific to the region. To calibrate expected levels of ground shaking for the scenarios, we use three recent events in the study area that have both ground motion data and intensity data (Modified Mercalli Intensity, MMI; Wood and Newmann 1931): moment magnitude (**M**)5.0 Val des Bois (VdB) June 2010, **M**3.9 Montreal (Mtl) October 2012, **M**4.5 Ladysmith (Ldy) May 2013. Information for these events is provided in Table 1 and their locations with respect to Montreal are shown in Fig. 1. In addition to the selected earthquakes, there was the **M**3.5 Gatineau earthquake that occurred on November 2012 close to the study area, but due to the smaller magnitude and a lack of felt reports for this event, we opted not to consider it in our validation exercise. Fig. 2 is a plot of vertical-component response spectra, (PSAv, the 5%-damped pseudo-acceleration) on rock sites, compared to the GMPEs for Eastern North America (ENA) proposed for hazard mapping for NBCC 2015 (Atkinson and Adams 2013; hereinafter referred to as AA13). Each of the three plotted GMPEs (central, upper and lower curves) is an alternative estimate of the median ground-motion amplitudes. The low and high curves express uncertainty about the central AA13 GMPE. Overall the GMPEs predict the observed data well, with Mtl following the “low” AA13 curve, Ldy following the central (“med”) AA13 curve, and VdB following the “high” AA13 curve (approximately).

**Table 1 – Recent events recorded at Montreal.**

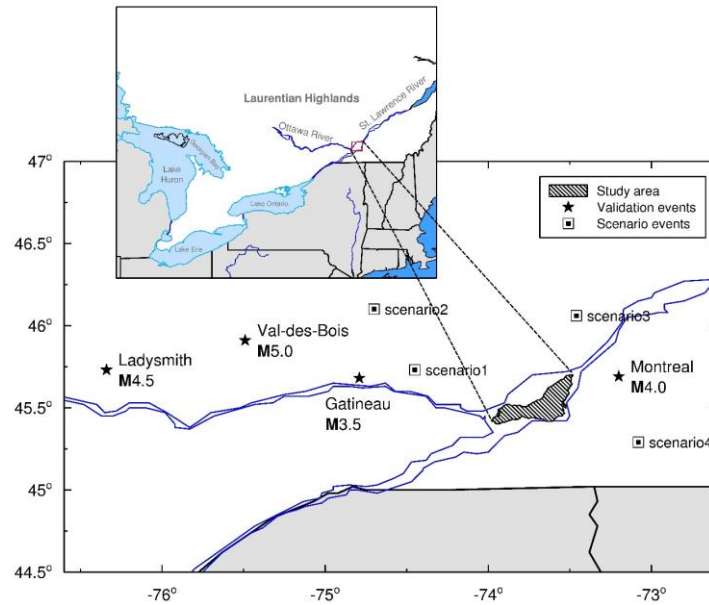
	Date	Hour	Lat.	Lon.	Depth (km)	MN	M	AA13 GMPE Level
Val des Bois	2010-06-23	17:41:41	45.91	-75.49	16.4	5.8	5.0	High
Montreal	2012-10-10	04:19:28	45.69	-73.20	21	4.5	3.9	Low
Ladysmith	2013-05-17	13:43:23	45.73	-76.34	20	5.2	4.5	Med
Gatineau	2012-11-06	09:05:28	45.68	-74.79	15	4.2	3.5	Med

After validating the accuracy of our shakemap technique using the selected events, we generate shakemaps for scenarios involving stronger shaking and greater damage potential. The target probability level for the scenarios is near the 2%/50 yr. ground motions, as used for design of new structures in Montreal according to the National Building Code of Canada (NBCC 2010). The NBCC (2010) indicates that Montreal can expect horizontal peak ground acceleration (PGA) of 0.43g with a probability of exceedance of 2%/50 yr; motions of this intensity could cause significant damage (Adams and Atkinson 2002; Adams and Halchuk 2003; Rosset and Chouinard 2009). Deaggregation from seismic hazard analysis shows that the main contribution to seismic hazard at the 2%/50 yr probability level, for short-to-intermediate periods, comes from the potential for earthquakes of M~5 to 6.5 at a distance of < 50 km (Atkinson and Goda 2011). The possible damage patterns are evaluated, considering several locations of hypothetical epicenters in and around the Montreal region.

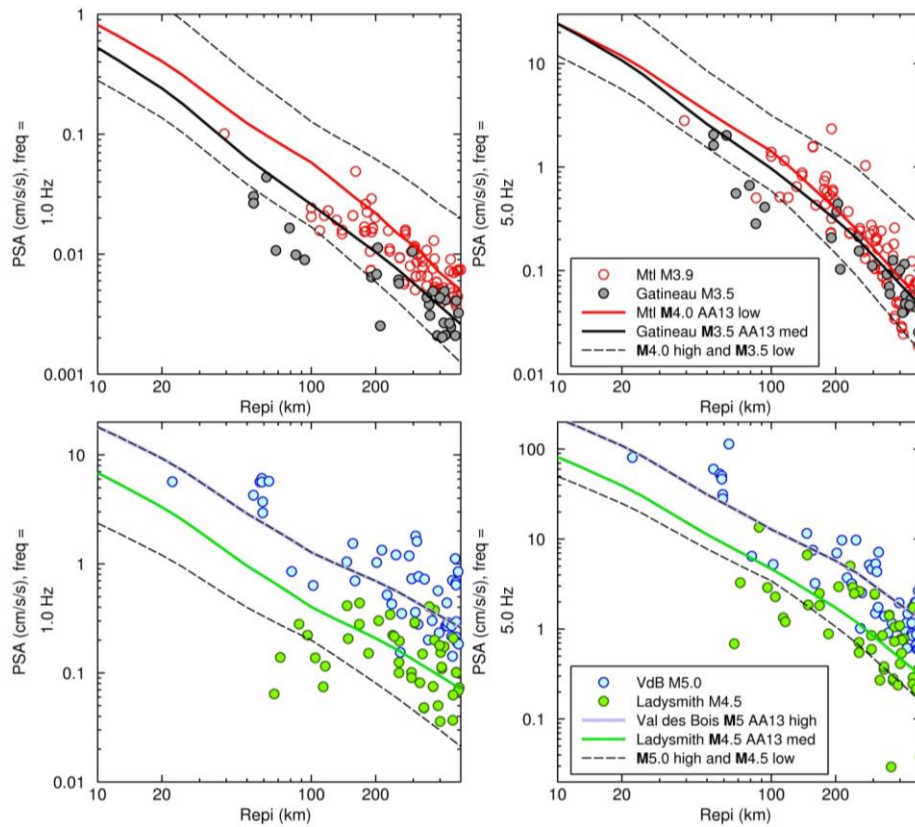
## 2. Recent Events in Study Area

Fig. 1 shows the geographical location and extent of the study area. Based on the exposed population and on the probability of earthquake occurrence, Montreal ranks second in Canada after Vancouver for seismic risk (Adams et al. 2002). The seismic activity in the region is attributed to the reactivation of ancient normal rift faults along the St. Lawrence and Ottawa Rivers as well as the passage of an ancient hot spot beneath the region (Adams and Basham 1991; Ma and Eaton 2007). The city is particularly vulnerable to seismic events since the city is largely built on recent unconsolidated marine and river deposits and much of its infrastructure is old and may have limited seismic resistance. Soft soil layers on the island of Montreal are mainly associated with thick Holocene-age Champlain Sea sediments (known as “Leda clay”; Hunter et al. 2002) and more recently sediments deposited from the Saint-Lawrence River. The island is located in a

moderate seismic zone where several earthquakes of intensity higher than MMI VI have occurred in the recent past (Lamontagne 2008).



**Fig. 1 – Map of the selected events for validation and four scenario events.**



**Fig. 2 – PSAv at 1 and 5 Hz on rock sites for M=3.5 to 5.0 events compared to AA13 GMPEs. The solid curve is the selected AA13 level for the event M to match the observations. Upper panels show M3.5 to 3.9 events, lower panels show M4.5 to 5.0 events. The dashed lines are the epistemic uncertainty range in the motions. For VdB, the dashed line is the same as the blue line.**

### 3. Construction of Shakemaps for the validation events

We construct the scenario shakemaps over a regular grid covering the Island of Montreal with a spacing of ~0.5 km. The soil stiffness is characterized by  $V_{S30}$ , the time-averaged shear-wave velocity over the top 30 m (Rosset et al. 2014). We consider five ground-motion parameters: the 5% damped pseudo-acceleration (PSA) at 1, 5 and 10 Hz, and PGA and peak ground velocity (PGV). In this study, the AA13 GMPEs for ENA were used to estimate median ground motions for a specified earthquake magnitude and distance. AA13 developed a “representative” or central GMPE based on alternative GMPEs and the data used to derive each model. Epistemic uncertainty in the best median curve was expressed by defining low and high GMPE variants about the central GMPE. For the validation, we have selected the low, med or high alternative for each of the three events as reported in Table 1. The ground motions for each event are defined for a reference NEHRP B/C boundary ( $V_{S30} = 760$  m/s). Once the median ground motions are estimated, we apply amplification factors to modify the ground motions for the likely effects of local soil conditions. In this study we use the Boore and Atkinson (2008; hereinafter referred to as BA08) site-amplification factors, for consistency with the AA13 GMPE formulation and the proposed approach for 2015 NBCC. The site amplification factor  $F_s$  is given by:

$$F_s = F_{LIN} + F_{NL} \quad (1)$$

where  $F_{LIN}$  and  $F_{NL}$  are the linear and nonlinear terms, respectively. The linear term is given by:

$$F_{LIN} = b_{lin} (V_{S30}/V_{ref}) \quad (2)$$

where  $b_{lin}$  is a period-dependent coefficient, and  $V_{ref}$  is the specified reference velocity, here 760 m/s, corresponding to NEHRP B/C boundary site conditions. The nonlinear term is given by:

$$\begin{aligned} F_{NL} &= b_{nl} (pga\_low/0.1) & pga4nl \leq a_1 \\ F_{NL} &= b_{nl} (pga\_low/0.1) + c [\ln(pga4nl/a_1)]^2 + d [\ln(pga4nl/a_1)]^3 & a_1 < pga4nl \leq a_2 \\ F_{NL} &= b_{nl} (pga4nl/0.1) & pga4nl > a_2 \end{aligned} \quad (3)$$

where  $a_1$  (= 0.03 g) and  $a_2$  (=0.09 g) are assigned threshold levels for linear and nonlinear amplification, respectively,  $pga4nl$  is the predicted PGA in g for  $V_{ref} = 760$  m/s, and  $pga\_low$  (=0.06 g) is a variable assigned to the transition between linear and nonlinear behaviors. The nonlinear slope  $b_{nl}$  is a function of both period and  $V_{S30}$  as given by:

$$\begin{aligned} b_{nl} &= b_1 & V_{S30} \leq V_1 \\ b_{nl} &= (b_1 - b_2) \ln(V_{S30}/V_2) / \ln(V_1/V_2) + b_2 & V_1 < V_{S30} \leq V_2 \\ b_{nl} &= b_2 \ln(V_{S30}/V_{ref}) / \ln(V_2/V_{ref}) & V_2 < V_{S30} < V_{ref} \\ b_{nl} &= 0 & V_{ref} \leq V_{S30} \end{aligned} \quad (4)$$

where  $V_1=180$  m/s,  $V_2=300$  m/s, and  $b_1$  and  $b_2$  are period-dependent coefficients.

As an example of how nonlinearity affects site amplification, Fig. 3 shows the amplification for PGV as function of  $V_{S30}$ , for suite of  $pga4nl$  values. It can be inferred from this figure that the amount of amplification on soft soil profiles can be ~4 times larger for weak motions in comparison to strong motions. Assuming that the amount of nonlinearity is controlled by the  $pga4nl$  from BA08, we would expect a large degree of nonlinearity for strong motions, thus greatly reducing motions. It is important to note that the motions in Montreal were relatively weak for the validation events and so the calculated  $pga4nl$  does not exceed the threshold level for linear amplification (i.e. 0.03 g). However, for the scenario events these nonlinear effects will be important.

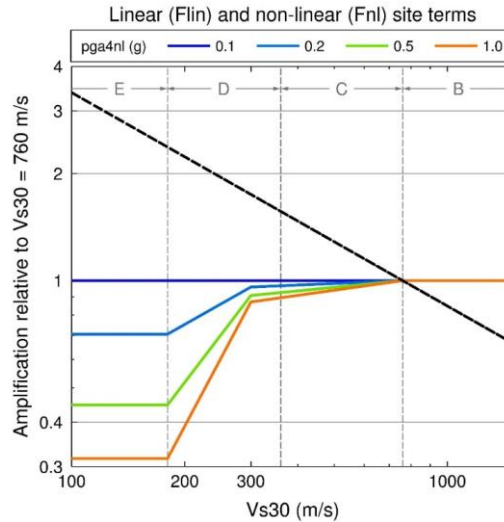


**Fig. 3 – Amplification for PGV as function of  $V_{S30}$ , for suite of pga4nl. Dashed black line shows the linear amplification and coloured lines show the nonlinear factor.**

We use Eqs. 2, 3, and 4 and  $V_{S30}$  values to estimate the expected amplifications at each point, using the pga4nl from BA08. The distance-scaling coefficients needed for the calculation of pga4nl and the site-amplification coefficients are the same as reported in Tables 3 and 6 in BA08.

Shakemaps for MMI, based on the median PGV (Atkinson and Kaka, 2007), are shown in Fig. 4. Note these are the median motions for each of the events, while in reality it is the motions above the median (i.e. those sites that experience larger-than-average motions) that dominate hazard and would strongly influence an actual shakemap. For this reason, in Fig. 4 we also plot the shakemap for median+sigma motions, where sigma expresses the aleatory uncertainty (i.e. random variability) of ground motions. We assume that the representative sigma values for a multi-site sigma would be about 0.27  $\log(10)$  units at low frequencies ( $\leq 1$  Hz), decreasing to 0.23 units at high frequencies ( $\geq 4$  Hz) (Atkinson and Adams 2013). Overall, by considering these figures we estimate intensities of III to V across Montreal for the VdB event (depending on site conditions), intensities of II to IV for the Mtl event, and intensities of I to III for Ldy.

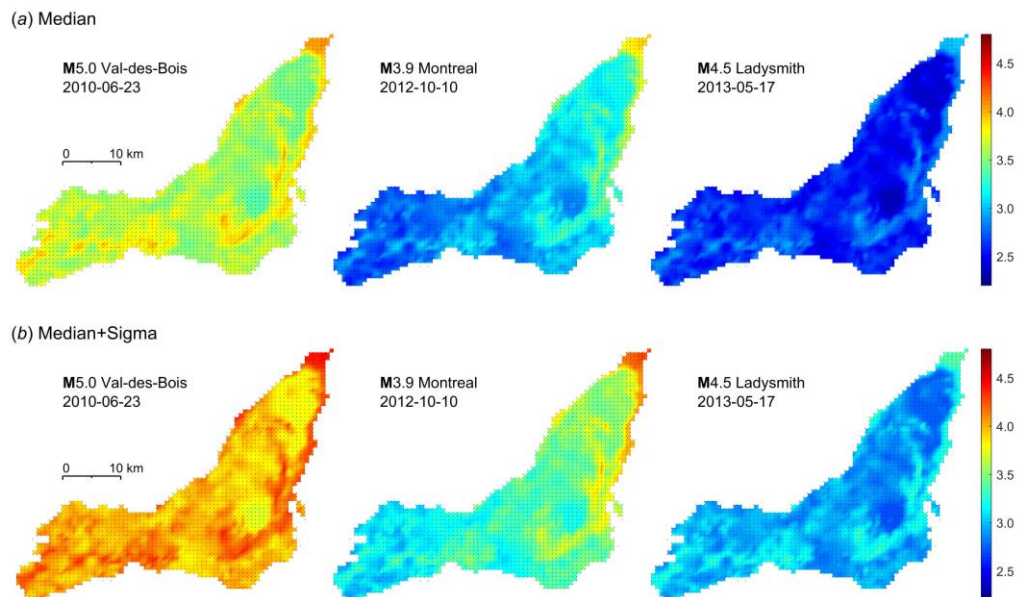


**Fig. 4 – Predicted MMI from PGV for the (a) median and (b) median+sigma motions due to the validation events (Val des Bois, Montreal, and Ladysmith earthquakes).**

#### 4. Comparing the predicted MMI to actual MMI for the validation events

Observed MMI were compiled by the Geological Survey of Canada using the individual reports from the DID YOU FEEL IT web application. Figure 5 shows the distribution of observations for the Mtl event. The average MMI is calculated in a regular grid of 1 km x1 km across Montreal and represented by a circle with a size proportional to its value.

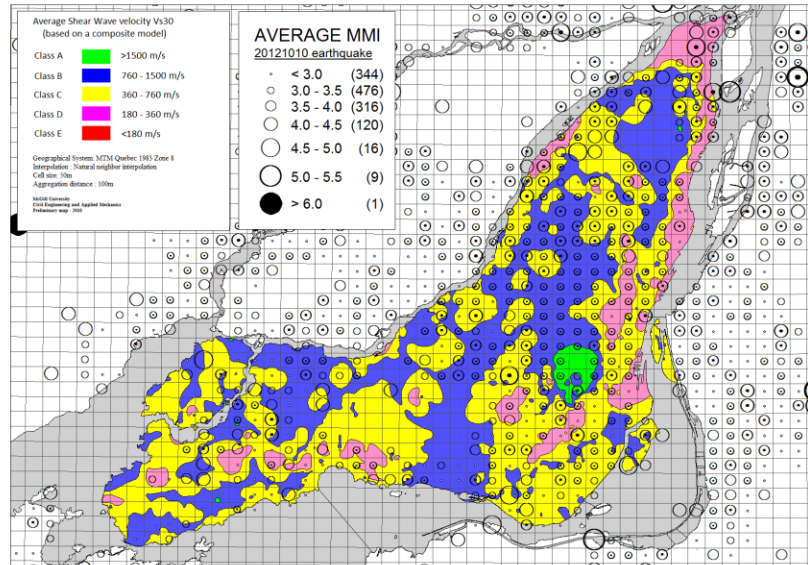


**Fig. 5 – Observed intensities for the M3.9 Mtl event. The central dot in the circle indicates a number of observations  $\geq 3$ . The number of observations is given in parentheses in the legend.**

In Table 2 we show the predicted MMI for the Montreal earthquake considering median (first row), and median+sigma (second row) GMPEs, in comparison to the observed MMI distribution (the two lines in red). We compare predicted MMI values only for the sites where we have observed intensity values and  $V_{S30}$  is known or has been reliably estimated. Predicted MMI values based on the median ground-motions are mostly centered on the second class ( $II < MMI \leq III$ ). However, the more realistic scenarios produced by adding random variability to the median ground motions, using the median+sigma motions, produces larger MMI values. Overall, the observed intensities are shifted to higher values than those predicted for median GMPE motions, illustrating the importance of larger-than-predicted observations in controlling reported intensity. Tables 3 and 4 show the same general results for the Val des Bois and Ladysmith events.

**Table 2 – Predicted MMI of the Mtl M4.0, compared to observed (the rows in red).**

Event	Number of points	MMI $\leq$ II	II<MMI $\leq$ III	III<MMI $\leq$ IV	IV<MMI $\leq$ V
<b>observed (<math>\geq 1</math> report)</b>	<b>411</b>	<b>4.4%</b>	<b>19.2%</b>	<b>66.9%</b>	<b>9.2%</b>
predicted (med)		-	41.4%	58.6%	-
predicted (med+sigma)		-	1.5%	94.9%	3.7%
<b>observed (<math>\geq 3</math> reports)</b>	<b>286</b>	<b>-</b>	<b>21.3%</b>	<b>73.8%</b>	<b>4.9%</b>
predicted (med)		-	32.2%	67.8%	-
predicted (med+sigma)		-	0.4%	95.8%	3.8%

**Table 3 – Predicted MMI of the VdB M5.0, compared to observed (the two rows in red).**

Event	Number of points	MMI $\leq$ II	II<MMI $\leq$ III	III<MMI $\leq$ IV	IV<MMI $\leq$ V
<b>observed (<math>\geq 1</math> report)</b>	<b>109</b>	<b>18.3%</b>	<b>29.4%</b>	<b>35.8%</b>	<b>14.7%</b>
predicted (med)		-	-	99.1%	0.9%
predicted (med+sigma)		-	-	49.5%	50.5%
<b>observed (<math>\geq 3</math> reports)</b>	<b>16</b>	<b>6.3%</b>	<b>68.8%</b>	<b>25.0%</b>	<b>-</b>
predicted (med)	16	-	-	100%	-
predicted (med+sigma)	16	-	-	43.8%	56.2%

**Table 4 – Predicted MMI of the Ldy M4.5, compared to observed (the row in red).**

Event	Number of points	MMI≤II	II<MMI≤III	III<MMI≤IV	IV<MMI≤V
observed (≥ 1 report)	46	78.3%	6.5%	15.2%	-
predicted (med)	46	-	100%	-	-
predicted (med+sigma)	46	-	30.4%	69.6%	-

We also compare the observed and predicted spectra for the seismograph stations or strong motion stations available within the grid. There is only one weak-motion seismograph station (MNTQ) in Montreal. Figure 6 compares observed and predicted motions for this site for the Mtl and Ldy events. Overall, the observed and predicted spectra are in reasonable agreement, considering a typical site-to-site random variability of about a factor of two. Figure 7 compares observed PSA with predicted (median) PSA for VdB at each strong-motion site. Overall, from the validation events we conclude that the ground motions appear to be reasonably well predicted by our GMPE and site amplification model.

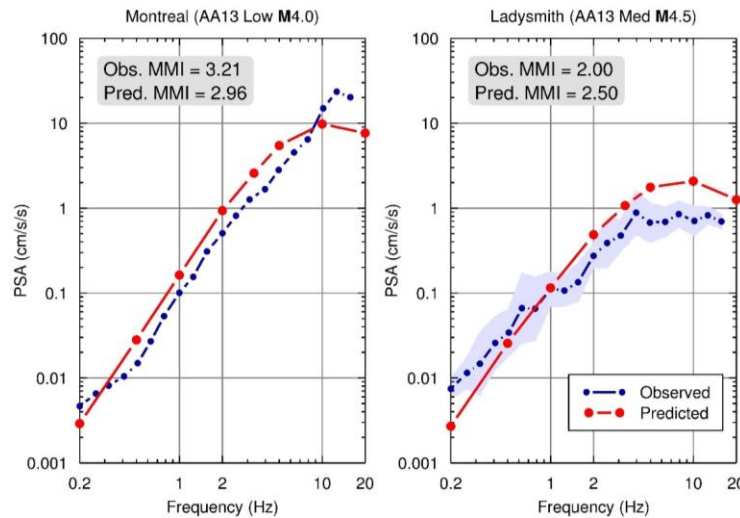


**Fig. 6 – Observed and predicted PSA for the Mtl and Ldy events at station MNTQ. The area enclosed by the two observed horizontal components for Ldy is shaded. MNTQ is at hypocentral distances of 44 km and 214 km from the Mtl and Ldy events, respectively and  $V_{S30} = 1087$  m/s.**

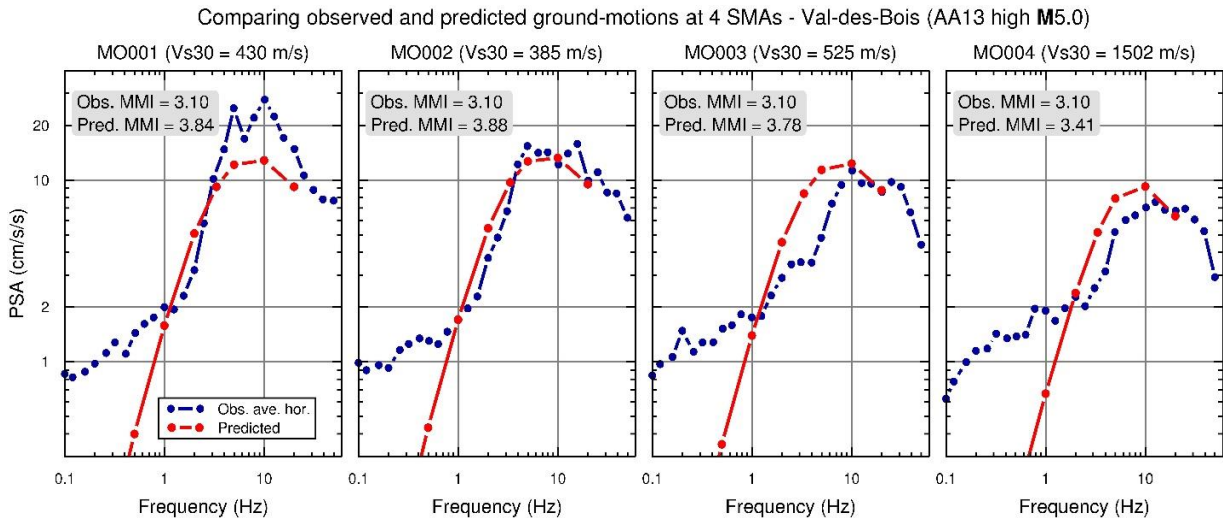


**Fig. 7 – Observed and predicted PSA at strong-motion sites for VdB (average horizontal component). All the strong-motion stations are at the hypocentral distances of 155-158 km.  $V_{S30}$  values (in m/s) for strong-motion stations MO001, MO002, MO003, and MO004 are 430, 385, 525, and 1502, respectively.**

## 5. Shakemaps for scenario events

### 5.1. Potential rupture scenarios

The method used for locating potential earthquake rupture scenarios in this study is one originally adapted for California (Tiampo et al. 2002; Tiampo et al. 2006). The idea is that changes in the background seismicity rate correspond to locations of ongoing stress change. The method identifies locations of both quiescence and activation. The activation signal is always larger in amplitude, but it has been suggested that areas that display both activation and quiescence together are more likely to produce an event (Mignan and Tiampo 2010). Here a region within about 125 km of Montreal was analyzed and an initial series of potential locations were selected based on this analysis technique for the period 2001-2011, as shown in Fig. 8. In this figure, locations of areas that are more active than the average background rate (seismic activation) are shown in red, those that are less active than the average background rate (seismic quiescence) are shown in blue.

While it is difficult to assign a probability value to the potential events, the technique does provide a means to evaluate the longer term stability of the locations and the anticipated magnitude based on approximate rupture dimension (Tiampo et al. 2006). As a result, we selected four scenarios, shown in Fig. 8, based on their location, magnitude, and likelihood. Scenario 1 was selected because it corresponds to the location of the Gatineau earthquake (Fig. 1), and it displays both activation and quiescence together. Scenario 2 was chosen because it has the largest potential magnitude of all the events shown in Fig. 8 and corresponds with the seismicity trend identified by Ma and Eaton (2007). Scenarios 3 and 4 were chosen because they represent moderate size events to the northeast and southeast of the city, locations with which we have limited prior experience. Historical records were used to assume reverse faulting as the most likely earthquake mechanism. However, note that the AA13 GMPEs do not depend on focal mechanism, and this does not affect the result.

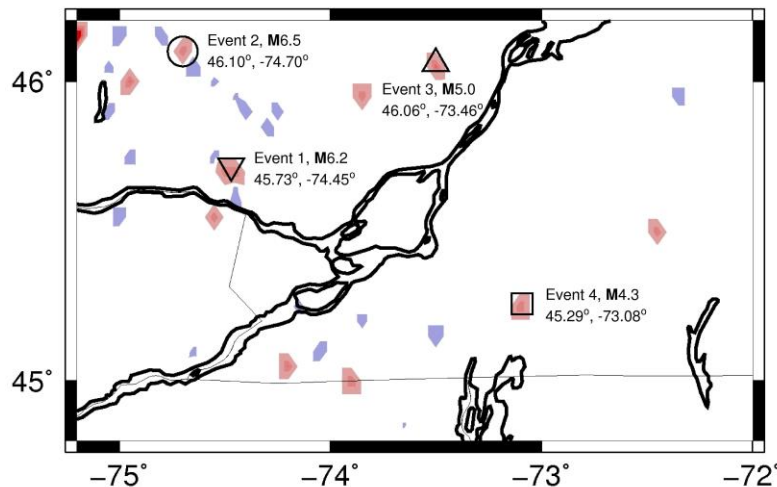


**Fig. 8 – Location of potential rupture scenarios (ranked from most likely to least likely). Shaded areas are local regions of seismic activation (red) and quiescence (blue). Scenarios (shown with symbols) have strikes of 315 to 335°, the depths are 14 to 16 km, and focal mechanisms are all considered to be reverse faulting.**

The expected intensity patterns for the four selected rupture scenarios (Fig. 8), are calculated following the procedure described for the other scenario events. For the sake of brevity, we only present results for Scenario 1 (Fig. 9). At each scenario location, we consider two hypothetical earthquakes with magnitudes of **M6.5** and **M7.0**; we used these magnitudes in order to produce stronger motions, close to the 2%/50 yr values as provided in NBCC. For each magnitude, two alternatives are considered to calculate motions as given by the AA13 median and high curves. For each shakemap, we also considered aleatory variability, as discussed for the validation events, by adding one sigma to the median GMPE curves. We recognize that these scenarios represent a range of events, including some extreme scenarios. This range is provided for illustration, to show the effects of magnitude and ground-motion level on the resulting predicted intensities.

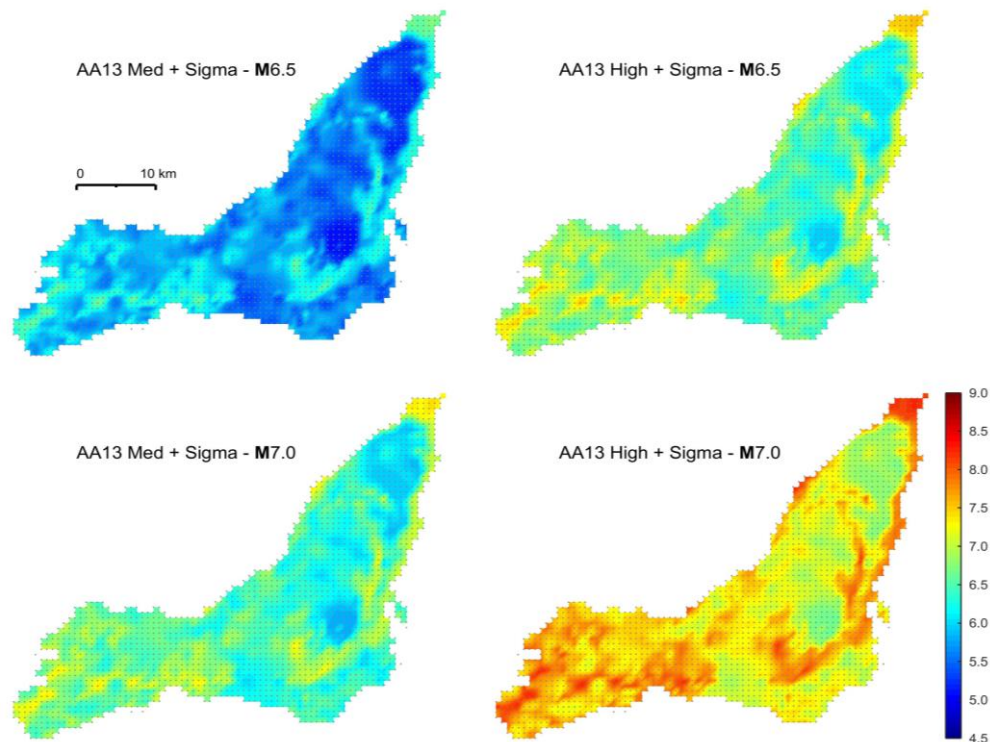


**Fig. 9 – Intensity (MMI) maps for the Scenario 1 from Fig. 8. All the shakemaps are plotted on the same colour scale (from blue for MMI 4.5 to red for MMI 9.0).**

## 6. Discussion and conclusions

The procedure used to generate the shakemaps for Montreal includes a GMPE validation phase that is based on observed intensity and ground motion data. The limited number of observations with  $\text{MMI} > \text{V}$  and ground motion above  $0.03g$  does not allow a robust validation. This results in significant uncertainty in the resulting shakemaps, a situation which will not be significantly improved until further recorded data are available. In this paper we did not introduce spatial correlation of ground-motion due to the added complexity this would introduce to a study that is largely exploratory, and focused at this time on the relative effects of ground motions and site amplifications. Nevertheless, we acknowledge the potential importance of spatial correlation in determining actual losses. The method of Tiampo et al. (2002, 2006), used to define potential earthquake sources, also needs to be refined with additional data; the potential rupture scenarios are very uncertain because the background seismicity is low, limiting statistical resolution. For the calculated scenarios with  $\text{M}7.0$  close to Montreal (Scenario 1), the maximum predicted MMI is around IX. Such a scenario is considered extreme, since the likelihood of such an event is very low, relative to typical building-code probabilities. The other scenarios with  $\text{M}6.5$  are more credible in this regard (e.g. Atkinson and Goda 2011); such scenarios would produce maximum MMI in the range of VII to VIII. An important point to note is that including random variability in ground-motions in a scenario event with  $\text{M}6.5$ , we would predict similar levels of ground-motions as for median ground-motions from a scenario  $\text{M}7.0$  event. Thus the overall level of shaking for the event is as important as its magnitude. Given the MMI distributions predicted by the scenario shakemaps, we would expect significant damage in some areas of Montreal, especially for vulnerable structures such as unreinforced masonry. This expectation accords with the seismic vulnerability analysis performed by Yu (2011).

## 7. Acknowledgements

Funding for this study from the Natural Sciences and Engineering Research Council of Canada (NSERC-CRSNG), and Canadian Seismic Research Network (CSRN) is gratefully acknowledged. We thank Trevor Allen for his helpful comments, which led to significant improvements in the manuscript.

## 8. References

- ADAMS, J., and ATKINSON, G.M. (2002), "Development of seismic hazard maps for the proposed 2005 National Building Code of Canada", *Can. J. Civil Eng.*, Vol. 30, pp. 255-271.
- ADAMS, J., and BASHAM, P.W. (1991), "The seismicity and seismotectonics of eastern Canada, In: Slemmons DB, Engdhal ER, Zoback MD, Blackwell DD (eds) Neotectonic of North America", Vol. 1, Geological Society of America, Boulder Colorado Decade Map.
- ADAMS, J., ROGERS, G., HALCHUCK, S., MCCORMACK, D., and CASSIDY, J. (2002), "The case of an advanced national earthquake monitoring system for Canada's cities at risk", *Proceedings of the 7<sup>th</sup> NCEE conference, Boston*, 10 pp.
- ADAMS, J., and HALCHUK, S. (2003), "Fourth generation seismic hazard maps of Canada: values for over 650 Canadian localities intended for the 2005 National Building Code of Canada", *OFR, GGC*, 4459.
- ATKINSON, G.M., and ADAMS, J. (2013), "Ground motion prediction equations for application to the 2015 Canadian National Seismic Hazard Maps", *Can. J. Civil Eng.*, Vol. 40, pp. 988-998.
- ATKINSON, G.M., and GODA, K. (2011), "Effects of seismicity models and new ground motion prediction equations on seismic hazard assessment for four Canadian cities", *Bull. Seismol. Soc. Am.*, Vol. 101, pp. 176-189.
- ATKINSON, G.M. and KAKA, S. (2007), "Relationships between felt intensity and instrumental ground motions for earthquakes in the central United States and California", *Bull. Seismol. Soc. Am.*, Vol. 97, pp. 497-510.
- BOORE, D.M. and ATKINSON, G.M. (2008), "Ground-motion prediction equations for the average horizontal component of PGA, PGV, and 5%-damped PSA at spectral periods between 0.01 s and 10.0 s", *Earthq. Spectra*, Vol. 24, pp. 99-138.
- HUNTER, J.A., BENJUMEA, B., HARRIS, J. B., MILLER, R.D., PULLAN, S.E., BURNS, R.A., and GOOD R.L. 2002. Surface and downhole shear wave seismic methods for thick soil site investigations. *Soil Dyn. Earthq. Eng.*, 22: 931-941.
- LAMONTAGNE, M. (2008), "Earthquakes in eastern Canada: a threat that can be mitigated", *Proceedings of the 4<sup>th</sup> Canadian conference on geohazards: from causes to management*, Locat, J (éd.); Perret, D (éd.); Turmel, D (éd.); Demers, D (éd.); Leroueil, S (éd.), pp. 13-24.
- MA, S. and EATON, D.W. (2007), "Western Quebec Seismic Zone (Canada): Clustered, mid-crustal seismicity along a Mesozoic hotspot track", *J. Geophys. Res.*, Vol. 112, pp. B06305.
- MIGNAN, A., and TIAMPO, K.F. (2010), "Testing the Pattern Informatics index on synthetic seismicity catalogues based on the Non-Critical PAST", *Tectonophysics*, Vol. 483, pp. 255-268.
- NATIONAL BUILDING CODE OF CANADA (NBCC) (2010), "National Research Council of Canada (NRCC)", Ottawa, Ontario. Volume 1, Division B, Part 4.
- ROSSET, PH., and CHOUINARD, L.E. (2009), "Characterization of site effects in Montreal, Canada", *Natural Hazards*, Vol. 48, pp. 295-308.
- ROSSET, PH., BOUR-BELVAUX, M., and CHOUINARD, L.E. (2014), "Microzonation models for Montreal with respect to  $V_{S30}$ ", *Bull. Earthq. Eng.*, DOI 10.1007/s10518-014-9716-8.
- TIAMPO, K.F., RUNDLE, J.B., KLEIN, W., HOLLIDAY, J. (2006), "Forecasting rupture dimension using the Pattern Informatics technique", *Tectonophysics*, Vol. 424, Issues 3-4, pp. 367-376.
- TIAMPO, K.F., RUNDLE, J.B., MCGINNIS, S., GROSS, S., KLEIN, W. (2002), "Mean-field threshold systems and phase dynamics: An application to earthquake fault systems", *Europhysics Letters*, Vol. 60, No. 3, pp. 481.
- WALD, D.J., QUITORIANO, V., HEATON, T.H., KANAMORI, H., SCRIVNER, C.W., and WORDEN, C.B. (1999), "'Trinet ShakeMaps': rapid generation of instrumental ground motion and intensity maps for earthquakes in Southern California", *Earthq. Spectra*, Vol. 15, pp. 537-556.
- WALD, D.J., WALD, L., WORDEN, B., and GOLTZ, J. (2007), "USGS ShakeMap-A tool for earthquake response", *U. S. Geol. Surv. Fact Sheet 087-03-508*, 4 pp.
- WOOD, H.O., and NEWMANN, F. (1931), "Modified Mercalli Intensity Scale of 1931", *Bull. Seismol. Soc. Am.*, Vol. 21, pp. 277-238.
- WORDEN, C.B., GERSTENBERGER, M.C., RHOADES, D.A., and WALD, D.J. (2012), "Probabilistic relationships between ground-motion parameters and modified Mercalli intensity in California", *Bull. Seismol. Soc. Am.*, Vol. 102, pp. 204-221.
- YU, K. (2011), "Seismic Vulnerability Assessment for Montreal - An Application of HAZUS-MH4", *Master Thesis*, McGill University, Montreal, Canada.